Rotational Spectra of Biomolecules: Histamine

Beat Vogelsanger, Peter D. Godfrey, and Ronald D. Brown*

Contribution from the Centre for High Resolution Spectroscopy and Opto-Electronic Technology, Chemistry Department, Monash University, Clayton, Victoria, Australia.
Received December 26, 1990

Abstract: The rotational spectrum of histamine has been observed in a free-expansion jet spectrometer in the range 59–64 GHz. Four species of histamine have been identified as the most stable conformers, all of them gauche, in contrast to results of X-ray and NMR solution studies. Parallel ab initio molecular orbital calculations (3-21G and 6-31G bases) indicate that 20 tautomer/conformer possibilities exist and helped to identify the 4 most stable conformers. Identification was based on rotational constants, inertial defects, dipole moment components, quadrupole hyperfine multiplets, and studies of the pentadeuterio derivative of histamine. All four of the identified conformers are gauche, one of the $N_{(1)}$-H tautomer and three of the $N_{(3)}$-H tautomer (in order of stability the conformers are G-IVa of $N_{(1)}$-H, G-Ib, G-Vc, and G-Ic of $N_{(3)}$-H (see Figure 2), the expanding beam being estimated to contain comparable amounts of the first two species and 40% and 30%, respectively, of the last two). All four species seem to be stabilized by some form of hydrogen bonding involving the amino group of the side chain.

Introduction

The biological significance of histamine, (2-aminoethyl)-imidazole,[1] is attested by a voluminous literature on this molecule. Its primordial activity at the central nervous system level and in the regulation of insomnia gave it a significance similar to that of adrenaline and acetylcholine. It is also a powerful vasodilator and a stimulator of gastric secretion in higher animals. Its biological activity has stimulated a number of studies of its tautomerism, its conformation, and its overall geometry, ranging from NMR studies in solution,[2] an X-ray crystallographic study,[3] and molecular orbital calculations of varying sophistication.[4] In the crystal, histamine is the trans conformer of histamine $N_{(1)}$-H[3] while in solution it appears to be roughly equal proportions of trans and gauche conformers of the $N_{(3)}$-H tautomer.[2] The molecular orbital calculations are not mutually entirely agreed as to the lowest energy tautomer/conformer, but the most elaborate ab initio calculations (Hartree-Fock SCF using the STO-3G basis) considered only the trans conformer, similar to that found in the X-ray studies of histamine.

Because the effect of the environment, crystal lattice or surrounding solvent, is unknown, we have set out to establish the most stable tautomer/conformer of the isolated molecule by detection and analysis of the rotational spectrum of histamine, the general style of the work being the same as that employed in our previous studies of biologically important molecules.[5] In parallel, we have also undertaken an extensive exploration of the energies of various tautomer/conformers using ab initio molecular orbital calculations and a more elaborate basis set (3-21G and 6-31G) than previously used.

Molecular Orbital Study

Calculations were performed on the histamine molecule by using the GAUSSIAN 88 package[6] and the 3-21G basis set. The primary structural features to be explored in order to determine the shape of histamine (i.e., its most stable tautomeric/conformational form) are the tautomerism of the imidazole ring and the three torsional parameters, τ_1, τ_2, and τ_3, defining the conformation with respect to the ethane skeleton, as illustrated in Figure 1. We anticipated that energy minima with respect to τ_2 would be found in the vicinity of the trans (T) (fully extended chair, $\tau_2 = 180°$) and gauche (G) (folded chair, $\tau_2 = 60°$ or 300°). This proved to be the case; all of our geometry optimizations, starting with arbitrary values of τ_2, ended with τ_2 values of 60°, 180°, or 300°. Variations in τ_3 indicated that stable conformers corresponded to values of this parameter representing staggered positions of the amino group. Variations of τ_1 indicated that the rotation of the imidazolyl group is much less restricted. In geometry optimizations, the imidazole ring was kept planar but all parameters were optimized. We noticed, for example, that the ring angle $C_{(5)}$–$C_{(4)}$–$N_{(3)}$ changed from about 110.2° for the $N_{(1)}$-H tautomer to around 106.3° for the $N_{(3)}$-H tautomer, scarcely affected by the side chain conformation (see Table I), but our attention was focused primarily on the overall shape, i.e., side chain conformation.

In all we have found 20 energy minima corresponding to the shapes illustrated in Figure 2. These include the sole minimum previously reported (T-c) although this conformer is predicted to be appreciably higher in energy than a number of others that we have now discovered. Table I lists the calculated total energies, dipole moments, optimized geometrical parameters and derived spectroscopic constants for each conformer.

For the trans conformers, we started with the X-ray crystallographic structural parameters,[2] the geometry optimizations being performed with the imidazole portion being constrained to planarity. The species of local minimum energy so derived (T-c) for both the $N_{(1)}$-H and $N_{(3)}$-H tautomers had values of τ_1 and τ_2 and of the other structural parameters that closely coincide with those obtained in STO-3G based calculations of Topiol et al.[3] However, with the larger basis set (3-21G) and also with 6-31G basis, the $N_{(3)}$-H tautomer is predicted to be more stable than the $N_{(1)}$-H tautomer, contrary to the results when the STO-3G basis is used.

In addition, we were able to detect two further trans species (T-a and T-b) for both tautomers, with different conformations of the amino group. These species differed from T-c by less than 7° in the values of τ_1 and τ_2 and by less than 2 kJ mol^{-1} in energy. For the $N_{(1)}$-H tautomer, T-b is 0.1 kJ mol^{-1} more stable than T-c. We did not search for further trans species with τ_1 significantly different from 60–70° because single-point calculations for the trans conformer (Figure 3) indicate that this range of τ_1

(1) Although the standard nomenclature for histamine is either 1*H*-imidazole-4-ethanamine or 1*H*-imidazole-5-ethanamine depending upon the tautomer considered, all previous papers dealing with theoretical calculations on histamine and also the biochemical literature adopt the numbering system used here, where the skeleton numbering does not change with tautomerism.

(2) Ganellin, C. R.; Pepper, E. S.; Port, G. N. J.; Richards, W. G. *J. Med. Chem.* **1973**, *16*, 610–616. Ham, N. S.; Casy, A. F.; Ison, R. R. *J. Med. Chem.* **1973**, *16*, 470–475. Byrn, S. R.; Graber, C. W.; Midland, S. L. *J. Org. Chem.* **1976**, *41*, 2283–2288. Reynolds, W. F.; Tzeng, C. W. *Can. J. Biochem.* **1977**, *55*, 576–578. Wasylishen, R. E.; Tomlinson, G. *Can. J. Biochem.* **1977**, *55*, 579–582.

(3) Bonnet, J. J.; Ibers, J. A. *J. Am. Chem. Soc.* **1973**, *95*, 4829–4833.

(4) Kang, S.; Chou, D. *Chem. Phys. Lett.* **1975**, *34*, 537–541. Topiol, S.; Weinstein, H.; Osman, R. *J. Med. Chem.* **1984**, *27*, 1531–1534. Gresh, N.; Claverie, P.; Pullman, A. *Theor. Chim. Acta* **1984**, *66*, 1–20. Smeyers, Y. G.; Romero-Sanchez, F. J.; Hernandez-Laguna, A. *J. Mol. Struct.: THEOCHEM* **1985**, *123*, 431–442; **1990**, *207*, 157–167. Topiol, S. *J. Comput. Chem.* **1987**, *8*, 142–148.

(5) Brown, R. D.; Godfrey, P. D.; McNaughton, D.; Pierlot, A. *J. Am. Chem. Soc.* **1988**, *110*, 2329–2330; *Chem. Phys. Lett.* **1989**, *156*, 61–63; *J. Am. Chem. Soc.* **1989**, *111*, 2308–2310. Vogelsanger, B.; Brown, R. D.; Godfrey, P. D.; Pierlot, A. P. *J. Mol. Spectrosc.* **1991**, *145*, 1–11.

(6) GAUSSIAN 88: Frisch, M. J.; Head-Gordon, M.; Schlegel, H. B.; Raghavachari, K.; Binkley, J. S.; Gonzalez, C.; Defrees, D. J.; Fox, D. J.; Whiteside, R. A.; Seeger, R.; Melius, C. F.; Baker, J.; Martin, R. L.; Kahn, L. R.; Stewart, J. J. P.; Fluder, E. M.; Topiol, S.; Pople, J. A. Gaussian, Inc., Pittsburgh, PA.

0002-7863/91/1513-7864$02.50/0

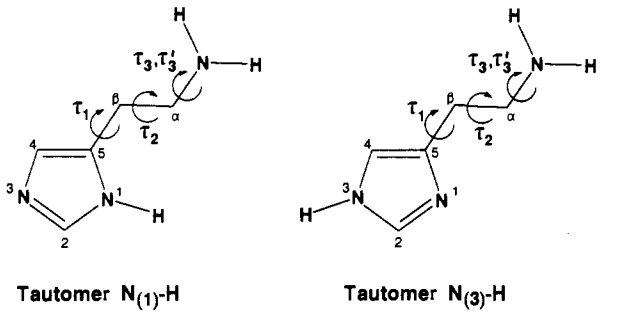

Figure 1. Parameters τ_1, τ_2, and τ_3 defining conformers of the histamine tautomers. Torsion angle τ_1 is viewed along the C_β–C_5 bond from C_β to C_5, τ_2 is viewed along C_α–C_β from C_α, and τ_3 and τ_3' are viewed along N–C_α bond from the amino nitrogen. All torsion angles are given clockwise with the "zusammen" position as origin.

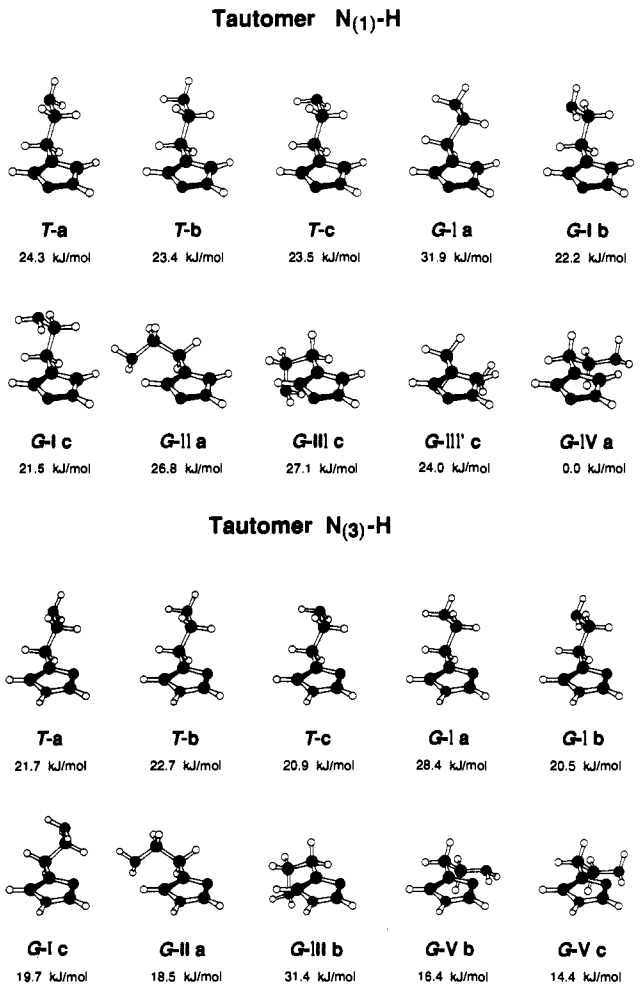

Figure 2. Twenty conformers corresponding to local energy minima for histamine tautomers $N_{(1)}$-H and $N_{(3)}$-H with relative energies (3-21G basis) included.

corresponds to the most stable conformer of this type and also our spectroscopic studies (see below) clearly show that none of the observed species has the trans conformation. The single-point calculations were performed for both tautomers and for all three preferred conformations of the amino group: (a) $\tau_3/\tau_3' = 60°/180°$, (b) 180°/300°, (c) 300°/60°. The total energy was computed at 30° increments of τ_1 covering 180° (because of the relationships T-a(360° − τ_1) = T-b(τ_1); T-b(360° − τ_1) = T-a(τ_1); and T-c(360° − τ_1) = T-c(τ_1), only a range of 180° of τ_1 needs to be covered). All other structural parameters were constrained to the optimum values found for the conformers T-a. The potential energy functions, obtained by fitting quartic spline interpolation functions, are shown in Figure 3.

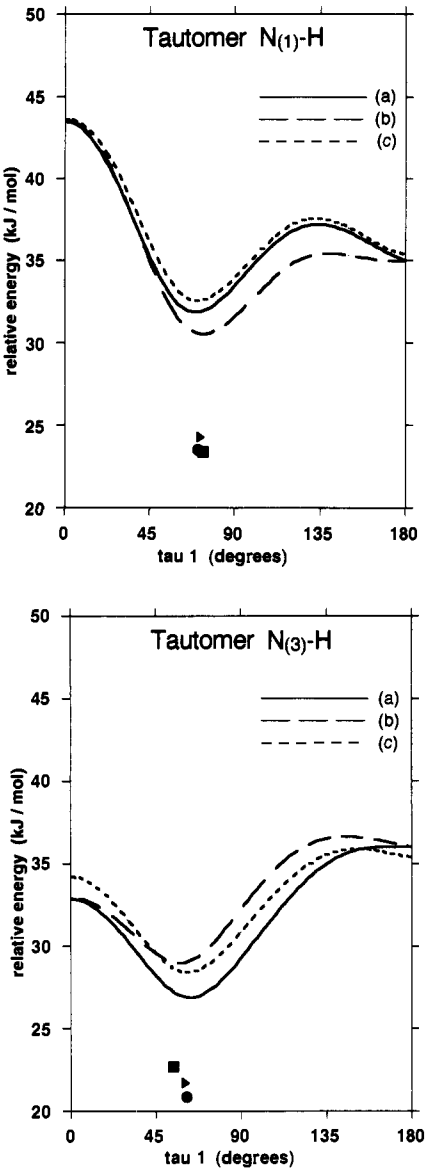

Figure 3. Potential energy functions for rotation about the aminoethyl CC bond (τ_1) in histamine for the trans conformers (τ_2 = 180°). The three graphs correspond to conformations of the amino group τ_3/τ_3' = 60°/180° (a), 180°/300° (b), and 300°/60° (c). The fully optimized energy minima are represented by triangles (a), rectangles (b), and circles (c).

In the case of the gauche conformer (τ_2 = 60°), single-point calculations were performed as just described for the trans conformer except that in this case the range of coverage of τ_1 had to be 360°. The potential energy functions are shown in Figure 4.

Because we wished to ensure that every minimum for a gauche conformer would be detected, we initiated complete geometry optimizations from each of these points in case a and from every second point in cases b and c. This procedure detected seven different gauche energy minima for each tautomer. Adjustments during these optimizations were up to 140° in τ_1 and up to 120° in τ_3 and τ'_3. Optimizations starting from up to eight different initial structures ended in the same minima.

For both tautomers, the shapes of the potential energy functions for (b) and (c) are seen (Figure 4) to be similar but quite different from the function for (a). The functions b and c have a maximum near 150°, which can be attributed to repulsion between the hydrogens of the amino group and the H located in $C_{(4)}$. In the case of the $N_{(1)}$-H tautomer, there is a maximum at $\tau_1 \approx 330°$ stemming from the repulsion between the amino hydrogens and the H at $N_{(1)}$. In the case of the $N_{(3)}$-H tautomer, the maximum

Table I. 3-21G-Optimized Parameters[a] for Histamine

	$N_{(1)}$-H tautomer									
parameter[b]	T-a	T-b	T-c	G-Ia	G-Ib	G-Ic	G-IIa	G-IIIc	G-III'c	G-IVa
$C_{(5)}$–$C_{(4)}$–$N_{(3)}$	110.2	110.2	110.2	110.1	110.1	110.2	109.9	110.1	110.1	109.7
τ_1	71.8	73.0	70.1	52.8	74.0	71.8	148.7	204.4	284.4	321.4
τ_2	179.5	182.1	179.9	52.8	66.4	60.6	64.9	63.8	61.2	66.1
τ_3	71.0	162.5	292.5	50.4	173.2	299.2	63.1	297.5	288.0	66.0
τ_3'	201.1	291.1	63.9	182.4	303.0	67.6	193.0	66.6	66.2	191.0
E_{rel}, kJ mol^{-1}	24.3	23.4	23.5	31.9	22.2	21.5	26.8	27.1	24.0	0.0
A, MHz	6729.1	6725.3	6677.9	4540.9	4598.3	4511.0	5087.9	4811.9	4609.1	4920.7
B, MHz	1043.2	1045.0	1040.5	1327.6	1327.0	1317.8	1337.1	1304.6	1388.1	1429.2
C, MHz	964.3	963.6	959.1	1278.9	1235.2	1248.3	1103.6	1164.5	1188.0	1159.6
Δ, uÅ^2	−35.5	−34.3	−34.4	−96.8	−81.6	−90.7	−19.4	−58.4	−48.3	−20.5
μ_a, D	3.2	3.2	2.6	4.4	2.1	1.6	2.9	0.5	2.6	6.1
μ_b, D	3.8	2.3	2.1	1.5	3.9	3.0	4.3	4.6	1.7	1.0
μ_c, D	0.3	0.3	1.9	2.1	1.5	0.6	0.2	1.3	2.4	0.3
μ_{tot}, D	5.0	3.9	3.8	5.1	4.6	3.4	5.2	4.8	3.9	6.2
$\Delta(A)$, MHz[c]	−964.5	−961.5	−949.8	−614.5	−584.7	−567.0	−520.9	−559.3	−608.3	−633.3
$\Delta(B)$, MHz[c]	−84.8	−84.2	−79.9	−90.1	−89.3	−78.5	−111.5	−91.5	−74.6	−97.9
$\Delta(C)$, MHz[c]	−88.4	−89.5	−85.7	−99.1	−91.1	−89.7	−94.3	−80.8	−85.7	−93.9
$\Delta(\Delta)$, uÅ^2[c]	−2.7	−1.3	−1.2	−11.9	−10.9	−9.0	−2.9	−10.7	−4.3	−2.7
	$N_{(3)}$-H tautomer									
parameter[b]	T-a	T-b	T-c	G-Ia	G-Ib	G-Ic	G-IIa	G-IIIb	G-Vb	G-Vc
$C_{(5)}$–$C_{(4)}$–$N_{(3)}$	106.3	106.3	106.3	106.2	106.2	106.3	106.1	106.3	106.4	106.4
τ_1	60.3	54.0	60.9	63.1	64.6	34.6	146.0	209.3	309.1	306.6
τ_2	181.7	182.3	183.4	67.8	67.6	56.1	64.9	68.3	74.2	68.3
τ_3	69.1	159.1	297.2	71.4	173.8	289.8	61.1	176.9	180.5	306.7
τ_3'	196.3	287.8	66.9	201.4	300.3	57.0	188.0	306.8	308.3	70.6
E_{rel}, kJ mol^{-1}	21.7	22.7	20.9	28.4	20.5	19.7	18.5	31.4	16.4	14.4
A, MHz	6724.1	6749.5	6656.5	4552.2	4565.3	4586.2	5052.1	4825.6	4971.5	4869.5
B, MHz	1057.3	1063.8	1056.1	1307.2	1319.5	1382.7	1353.2	1299.7	1388.9	1392.3
C, MHz	967.2	963.1	964.1	1251.6	1261.6	1247.0	1113.0	1185.1	1142.2	1145.5
Δ, uÅ^2	−30.6	−25.2	−30.2	−93.8	−93.1	−70.4	−19.4	−67.1	−23.1	−25.6
μ_a, D	2.7	2.7	3.3	0.9	2.6	4.3	0.9	1.6	4.1	4.5
μ_b, D	0.9	2.1	2.9	2.4	1.9	2.1	3.1	4.3	1.3	2.1
μ_c, D	1.2	2.2	0.1	0.2	0.9	1.7	0.2	1.5	1.9	0.2
μ_{tot}, D	3.1	4.1	4.4	2.6	3.4	5.1	3.2	4.8	4.7	4.9
$\Delta(A)$, MHz[c]	−801.4	−810.6	−785.1	−529.0	−523.0	−542.6	−501.1	−522.8	−569.5	−538.3
$\Delta(B)$, MHz[c]	−105.9	−106.0	−101.0	−118.2	−111.0	−108.6	−122.1	−106.7	−114.8	−111.6
$\Delta(C)$, MHz[c]	−100.0	−101.4	−97.8	−119.1	−107.7	−100.4	−100.7	−98.6	−105.5	−101.4
$\Delta(\Delta)$, uÅ^2[c]	−3.1	−1.1	−1.6	−10.5	−12.1	−10.5	−2.9	−8.8	−0.9	−1.7

[a] Fully optimized molecular geometry (imidazole portion kept planar), calculated with the 3-21 G basis set of the GAUSSIAN 88 packages. Only the most important geometrical parameters determining the molecular conformation are given in this table. [b] Bond angles and dihedral angles are in degrees. [c] Changes in rotational constants and inertial defect on deuterium to histamine-d_5 (for details see text).

near 330° of the function a can be explained by the repulsion between the two lone pairs of $N_{(1)}$ and the amino nitrogen.

Perhaps more interesting is the observation, from inspection of the shapes of the locally stable conformers displayed in Figure 2, that for many of the gauche conformers (but not the trans) their stability may be attributed to some form of hydrogen bonding involving the amino group of the side chain.

The species of lowest energy, G-IVa of the $N_{(1)}$-H tautomer, can form a hydrogen bond between the hydrogen on $N_{(1)}$ and the lone pair of the amino nitrogen. The two species G-Vc and G-Vb of the other tautomer can form a hydrogen bond between one of the amino hydrogens and the lone pair now on $N_{(1)}$. They are calculated to be 14.4 and 16.4 kJ mol^{-1} higher in energy but are the second and third most stable species.

For the species with $\tau_1 \approx 60°$, it appears that G-Ib and G-Ic can form a hydrogen bond between one of the amino hydrogens and the π-electron system of the imidazole ring. This yields an energy 8–11 kJ mol^{-1} lower than that for the G-Ia conformers, which are not able to form such a hydrogen bond. The conformers G-IIIb, G-IIIc, and G-III'c also appear to be stabilized by such a hydrogen bond between amino hydrogens and the π-electron system.

The conformers G-IIa seem to be stabilized by a hydrogen bond between the hydrogen on $C_{(4)}$ and the lone pair of the amino nitrogen. Experimental evidence for hydrogen bonding involving aromatic CH was first presented in 1963,[7] involving polyhalosubstituted benzenes. We are not aware of previous evidence for hydrogen bonding involving imidazole CH, but we note that the hydrogen in question here is unusually acidic, as demonstrated by the ease with which we have been able to exchange it with deuterium (see below).

Table II. Relative Energies (kJ mol^{-1}) of Different Species of Histamine, Calculated with 3-21G and 6-31G Basis Sets

species	3-21G	6-31G
	Histamine $N_{(1)}$-H	
T-a	24.3	16.7
G-Ia	31.9	23.4
G-Ib	22.2	15.0
G-Ic	21.5	15.0
G-IVa	0	0
	Histamine $N_{(3)}$-H	
T-a	21.7	12.3
G-Ib	20.5	11.3
G-Ic	19.7	11.6
G-Vb	16.4	10.6
G-Vc	14.4	10.3

For some of the 3-21G minima, geometry optimizations were repeated with the larger 6-31G basis set. The relative energies obtained from these more elaborate calculations are compared with the 3-21G energies in Table II. The energy differences between the species of lowest energy (G-IVa) and all other species are about 4–10 kJ mol^{-1} smaller than were found in the 3-21G-based calculations. Other features, described above for the 3-21G calculations, recur in the 6-31G calculations, e.g., the higher

(7) Allerhand, A.; von Ragué Schleyer, P. *J. Am. Chem. Soc.* **1963**, *85*, 1715–1723.

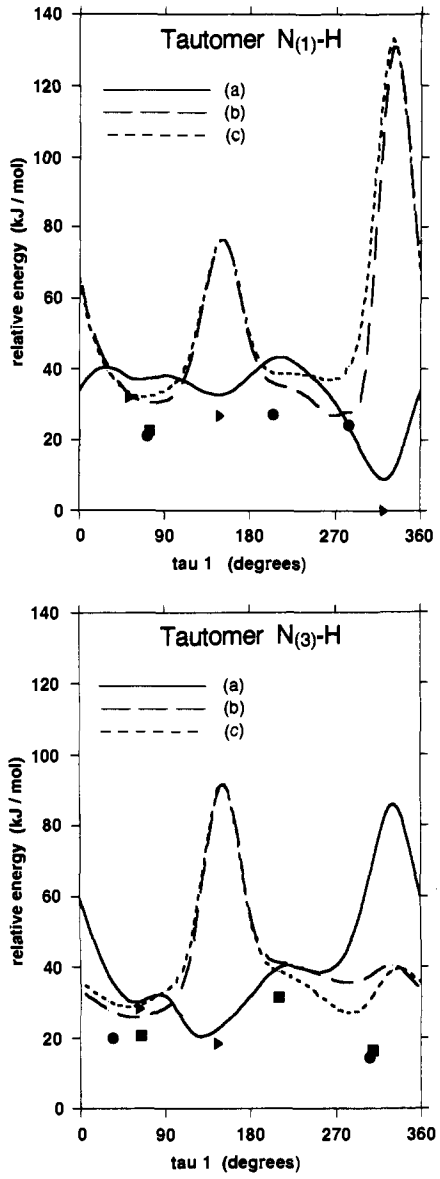

Figure 4. Potential energy functions as specified in Figure 3 but for the gauche conformers ($\tau_2 = 60°$).

stability of the G-Ib and G-Ic species as compared with G-Ia. For the latter species of the $N_{(3)}$-H tautomer, optimization actually led to G-Ib. Changes in dihedral angles were up to 5° for τ_1 or τ_2 and up to 10° in τ_3 except for G-Ic of the $N_{(3)}$-H tautomer, where τ_1 changed by 25.6°. Consequently all relevant parameters, such as rotational constants, inertial defects, dipole moment components, and quadrupole coupling constants, calculated with the 6-31G basis were very close to the respective 3-21G values, except for G-Ic of $N_{(3)}$-H, where all of these parameters substantially alter.

Experimental Details

The free-jet expansion, Stark-modulated spectrometer used in the present study has been described previously.[8] It is based on observing absorption in a supersonic expanding plume of histamine vapor entrained in argon. The stagnation pressure of the argon was typically 0.3 atm, the expansion producing rotational temperatures around 20 K. Our previous studies with this spectrometer showed no sign of spectral lines attributable to argon complexes, and likewise in the present work all observed lines were attributable to isolated histamine tautomers. The source was a phase-locked mm-wave klystron or a K-band klystron with tripler. Stark modulation at voltages up to 6000 V was employed at a plate separation of 3.5 cm. Accurate line frequencies were obtained by repetitive scans using a data-collection system based on a VAX 11/780 computer.

The optimum temperature for the solid sample compartment and inlet system was 130°, the argon being bubbled through the melted sample before being expanded through a nozzle 500 μm in diameter, the evaporation rate being about 0.2 g h^{-1}. At this temperature, there was almost no decomposition of the sample whereas for runs conducted at higher temperatures the sample needed regular replacement (e.g., at 180 °C replacement was necessary every 3–4 h). The spectrum was scanned over the range 59–64 GHz. The histamine was purchased from Sigma either as free base or as hydrochloride. The latter was converted to the free base by dissolving it in methanol and adding methanolic KOH.

A deuterated species was produced by first exchanging the three N-protons of the free base in heavy water at 20 °C for 24 h. After three repetitions, the NMR spectrum showed no trace of NH protons, whereas all aromatic and aliphatic CH protons were present. The microwave spectrum of this sample was quite weak, and from subsequent evidence it was apparent that histamines with differing degrees of deuterium up to d_5 had been formed in the heated sample compartment and inlet system. However, by bubbling heavy water vapor in argon through the melted sample before observing the spectrum, a sample highly enriched in an isotopomer that was found by NMR and by its microwave spectrum to be a pentadeutero isotopomer, with both amino hydrogens and the three imidazole ring hydrogens replaced by deuterium, was obtained.

Results and Discussion

The supersonic jet spectrometer converts what would otherwise be an exceedingly crowded and complex spectrum into a more tractable spectrum because of the depopulation of more highly excited rotational states at the low rotational temperatures achieved in the jet expansion. Nevertheless, approximately 200 transitions were observed in the range scanned. It proved possible to assign every one of these transitions to spectra of four different conformers/tautomers (C/T1–C/T4). The spectrum was dominated by high-J (J = 22–27) a-type transitions of C/T1 and low-J (J = 6–12) b-type transitions of C/T2. The b-type transitions of C/T1, 3, and 4 were found to be appreciably weaker while the a-type transitions of C/T2–4 were weaker again. The rotational constants derived from the four assigned spectra are listed in Table III. From a comparison with rotational constants calculated from geometries estimated from molecular orbital calculations (or geometrical data from the X-ray study), we can definitively exclude a trans conformation for all four C/T's because a trans conformation would give rise to values of $A \approx 6500$–7000 MHz, $B \approx 1000$–1100 MHz and $C \approx 900$–1000 MHz for the full range of possible τ_1 values.

Inertial Defect. The values of the inertial defect ($\Delta = I_c - I_a - I_b$), given in Table III, indicate that for C/T1 the heavy atoms must lie close to the plane of the imidazole ring. For a gauche conformation with $\tau_2 = 60°$, values of τ_1 in the vicinity of either 150° or 330° are required to produce an inertial defect around −22.3 μÅ², while the observed value of $\Delta = -36.8$ μÅ² for C/T3 corresponds to $\tau_2 = 60°$ and τ_1 around 0°, 120°, 180°, or 300°. In the case of C/T2 and C/T4, the inertial defects indicate that the heavy atoms of the side chain must be as far as possible out of the plane of the imidazole ring. For a gauche conformation ($\tau_2 = 60°$), τ_1 needs to be around 60° or 240°.

Stark Effect. For all four species, Stark effect measurements were performed for the low-J (J = 8–12) μ_b-type transitions. These exhibited both linear and quadratic Stark effects, the former dependent mainly on μ_a and the latter predominantly on μ_b and μ_c. The values of μ_a and $(\mu_b^2 + \mu_c^2)$ were determined from up to 30 measurements on individual Stark lobes. Results appear in Table III. Comparison of line intensities clearly indicated that for all species μ_b must be at least twice as large as μ_c.

From these dipole moment values and the observed relative line intensities, we were able to estimate the relative abundances of the four species of histamine. We conclude that C/T1 and C/T2 had about the same beam concentration whereas C/T3 and C/T4 were at a level of 40% and 30%, respectively, of the concentration of C/T1 or C/T2. If we assume a vibrational temperature of 400 K, corresponding to no vibrational cooling, the relative energy of C/T3 and C/T4 would be 3 and 4 kJ mol^{-1}, respectively, higher in energy than C/T1 or C/T2. Since there is likely to be some

(8) Brown, R. D.; Crofts, J. G.; Godfrey, P. D.; McNaughton, D.; Pierlot, A. P. *J. Mol. Struct.* **1988**, *190*, 185–193.

Table III. Derived Spectroscopic Parameters[a] for Histamine

parameter	C/T1	C/T2	C/T3	C/T4
A, MHz	4952.3184 (60)	4506.4569 (81)	4763.4588 (42)	4482.230 49 (85)
B, MHz	1391.9163 (12)	1332.1521 (34)	1373.5674 (28)	1313.1339 (36)
C, MHz	1141.191 16 (76)	1273.1066 (42)	1155.8093 (37)	1272.5341 (24)
D_J, kHz	0.133 29 (36)	0.4616 (32)	0.2673 (20)	0.4998 (13)
D_{JK}, kHz	−0.2676 (60)	2.2726 (76)	0.4221 (58)	2.9125 (58)
D_K, kHz	2.024 (85)	0.545 (96)	6.913 (47)	[b]
d_1, kHz	−0.026 88 (29)	0.022 30 (72)	0.005 98 (98)	0.0458 (15)
d_2, kHz	−0.002 39 (13)	−0.017 30 (50)	−0.018 98 (72)	0.022 11 (50)
rms error, kHz	29	32	25	22
no. of lines	39	26	33	26
Δ, uÅ^2	−22.278	−94.550	−36.775	−100.472
rel beam concn, %	100	100	40	30
$E_{rel}(T_{vib}$ = 400 K), kJ mol^{-1}	0	0	3	4
μ_a, D[c]	5.38 (4)	2.32 (2)	3.94 (2)	3.08 (3)
$(\mu_b^2 + \mu_c^2)^{1/2}$, D[c]	0.87 (6)	1.84 (2)	1.80 (3)	2.91 (3)
μ_{tot}, D[c]	5.45 (5)	2.96 (3)	4.33 (3)	4.24 (4)
$\Delta(A)$, MHz	−633.96	−514.54		
$\Delta(B)$, MHz	−96.93	−110.65		
$\Delta(C)$, MHz	−93.71	−106.27		
$\Delta(\Delta)$, uÅ^2	−2.54	−12.67		

[a] Numbers in parenthesis represent the standard deviation of the fit. [b] Statistically not significant parameter (F-test, 99% confidence interval). [c] From Stark effect measurements. The field was calibrated with the 4_{13}–4_{05} transition of SO_2 by using the dipole moment μ_b = 1.633 05 (4) D (Lovas, F. J. *J. Phys. Chem. Ref. Data* **1985**, *14*, 395–488).

vibrational cooling, such figures must be regarded as upper limits.

Hyperfine Splittings. Whereas none of the strong transitions (neither the low-J μ_b-type nor the high-J μ_a-type) exhibit nuclear quadrupole splitting, some hyperfine multiplets could be resolved for a few of the weakest lines (μ_b-type with $J \approx 14$–22). For each of the four detected species (C/T1–4) the nuclear quadrupole hyperfine patterns of at least five different transitions belonging to two or three different series were nevertheless sufficiently resolved that we were able to make fruitful comparisons with multiplet shapes computed ab initio for the twenty possible conformer/tautomers of histamine. Since histamine contains three inequivalent nitrogens, the expected hyperfine patterns can be extremely complicated. With estimates of the three sets of coupling constants derived from our molecular orbital calculations (see Table IV) and a version of our QUAD 4 code,[9] we derived simulated multiplets for comparison with observation. These comparisons were sufficiently conclusive that we could identify C/T1–3 purely from the hyperfine pattern studies. The coincidence between observed and calculated multiplets was very good when a 3-21G basis was used and excellent when a 6-31G basis was used in the calculations, with calculated splitting frequencies differing by less than 15% from the observed ones. This is in harmony with the kinds of agreement found for nitrogen hyperfine structures earlier by Brown and Head-Gordon.[10]

For C/T4, however, we could not find entirely satisfactory agreement between experimental and theoretical patterns for any of the species. Of those species with $\Delta_{calc} > 40$, only G-Ia and G-III'c of histamine $N_{(1)}$-H could be clearly excluded.

Histamine-d_5. Spectra of species analogous to C/T1 and C/T2 could be assigned. They showed the same characteristics as the spectra from the parent histamine (i.e., relative line intensities, characteristic bandheads, and Stark effects). The results are reported in Table III in the form of changes in the rotational constants.

Because the spectra for histamine-d_5 were approximately 3 times weaker than those of the parent molecule, the weaker spectra to be expected for C/T3 and C/T4 could not be observed with the current spectrometer sensitivity.

Identification of Species. From comparison of spectroscopic constants, dipole moment components, and changes in rotational constants on deuteration, it was straightforward to identify C/T1 with G-IVa of the $N_{(1)}$-H tautomer and C/T2 with G-Ib of the $N_{(3)}$-H tautomer (see Tables I, III, and IV). The identification of C/T3 with G-Vc of the $N_{(3)}$-H tautomer appears very likely. The study of hyperfine patterns independently leads to the same identifications (see Figure 5) and in particular confirms the identification of C/T3 as G-Vc. The remaining species is not so clearly identified by the evidence presently available, but it is likely to be G-Ic of the $N_{(3)}$-H tautomer because of excellent coincidence of the experimental rotational constants, inertial defect, and dipole moment components with values calculated for this species with a 6-31G basis set. The possibility that it could be a vibrational satellite of C/T2 (the rotational constants of C/T4 and C/T2 and

Table IV. 6-31G-Optimized Parameters[a] for the Four Species of Histamine That Were Identified To Be C/T1–C/T4

parameter[b]	histamine $N_{(1)}$-H G-IVa (C/T1)	histamine $N_{(3)}$-H G-Ib (C/T2)	G-Vc (C/T3)	G-Ic (C/T4)
$C_{(\beta)}C_{(5)}$	149.5	149.3	149.4	149.2
$C_{(\alpha)}C_{(\beta)}$	153.3	153.2	154.4	154.1
$NC_{(\alpha)}$	146.5	145.6	145.2	145.0
HN	99.9	99.5	99.7	99.4
H'N	99.7	99.6	99.6	99.5
$C_{(\beta)}C_{(5)}N_{(1)}$	122.7	121.3	122.1	121.1
$C_{(\alpha)}C_{(\beta)}C_{(5)}$	113.9	113.2	113.7	113.1
$NC_{(\alpha)}C_{(\beta)}$	111.0	110.9	115.4	115.4
$HNC_{(\alpha)}$	114.5	115.8	114.2	116.2
$H'NC_{(\alpha)}$	114.9	115.3	114.9	116.7
$C_{(\alpha)}C_{(\beta)}C_{(5)}N_{(1)}$ (τ_1)	318.7	68.8	302.0	60.2
$NC_{(\alpha)}C_{(\beta)}C_{(5)}$ (τ_2)	67.7	65.5	69.6	62.4
$NHC_{(\alpha)}C_{(\beta)}$ (τ_3)	66.3	164.0	305.0	287.4
$H'NC_{(\alpha)}C_{(\beta)}$ (τ_3')	197.2	298.5	76.5	65.5
rel energy, kJ mol^{-1}	0	11.3	10.3	11.6
A, MHz	4982.3	4617.8	4918.6	4562.9
B, MHz	1398.9	1306.9	1363.8	1291.5
C, MHz	1143.5	1239.7	1134.3	1256.1
Δ, uÅ^2	−20.7	−88.5	−27.8	−99.7
μ_a, D	6.0	2.4	4.2	3.4
μ_b, D	1.1	2.3	2.1	3.3
μ_c, D	0.4	0.7	0.2	0.3
μ_{tot}, D	6.1	3.3	4.7	4.8
$\chi_{aa}(N_{(1)})$, MHz	1.017	1.191	−0.619	0.882
$\chi_{bb}(N_{(1)})$, MHz	1.228	−2.816	−0.865	−2.742
$\chi_{aa}(N_{(3)})$, MHz	−3.648	0.714	1.134	0.727
$\chi_{bb}(N_{(3)})$, MHz	1.683	0.825	1.217	1.257
$\chi_{aa}(N)$, MHz	−3.443	2.106	−0.416	−2.032
$\chi_{bb}(N)$, MHz	1.337	−0.438	2.195	0.753

[a] Fully optimized molecular geometry (imidazole portion kept planar), calculated with the 6-31G basis set of the GAUSSIAN 88 package. Only the geometrical parameters of the aminoethyl side chain are given in this table. N denotes the amino nitrogen, H and H' the two amino hydrogens. [b] Internuclear distances are in picometers; bond angles are in degrees.

(9) Blackman, G. L.; Bolton, K.; Brown, R. D.; Burden, F. R.; Mishra, A. *J. Mol. Spectrosc.* **1973**, *47*, 457–468. Modernized and improved by P. D. Godfrey.

(10) Brown, R. D.; Head-Gordon, M. *Mol. Phys. 61*, 1183–1191.

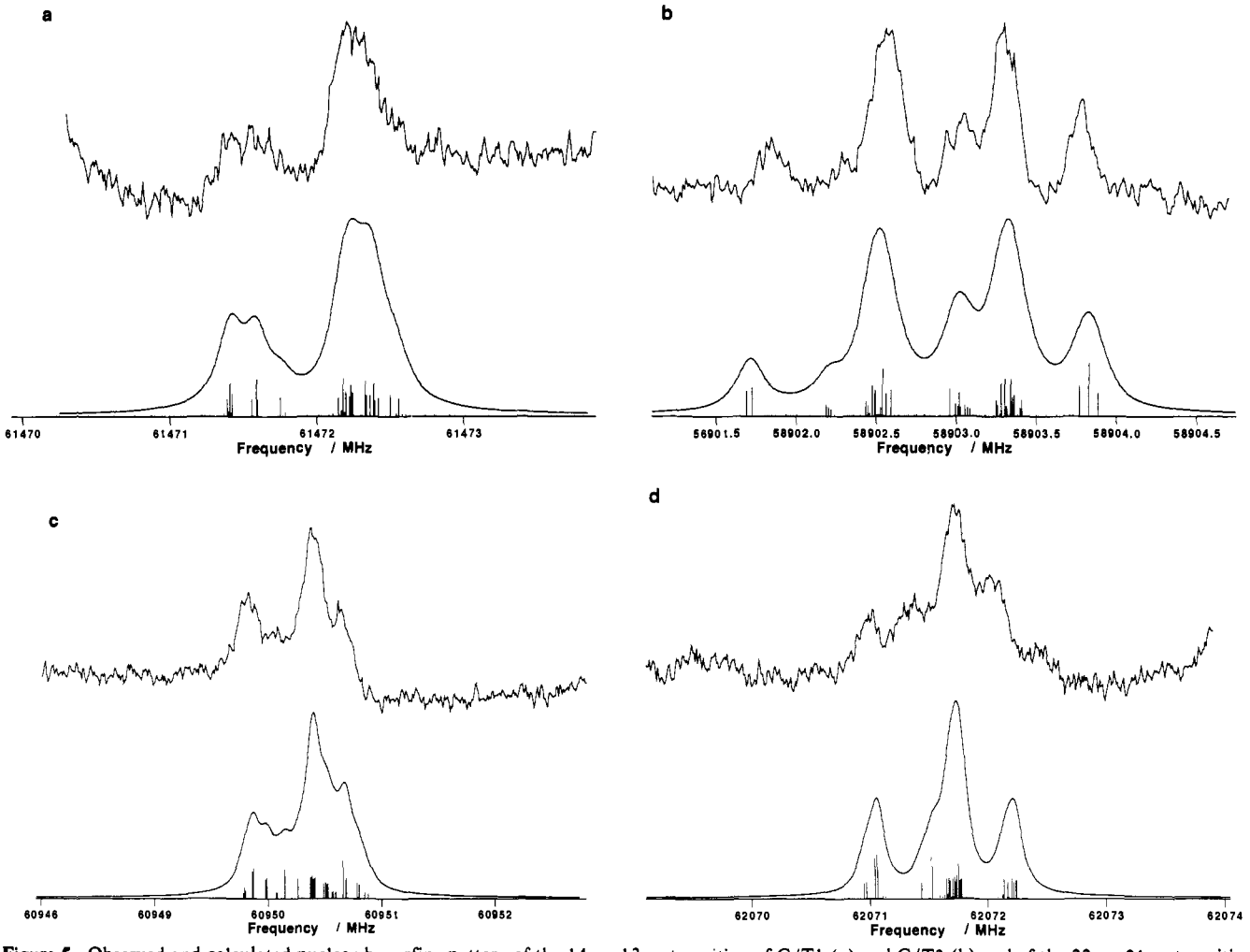

Figure 5. Observed and calculated nuclear hyperfine pattern of the $14_{3,11}$–$13_{3,12}$ transition of C/T1 (a) and C/T3 (b) and of the $22_{2,21}$–$21_{1,20}$ transition of C/T2 (c) and C/T4 (d). The calculated patterns are based on the ab initio values of the coupling constants given in Table IV.

their inertial defects are similar and appreciably different from those of C/T1 and C/T3) seems unlikely because the extent of the change in dipole moment components is greater than is usually observed for vibrational satellites, but the observed hyperfine patterns would agree slightly better with predictions in this case.

It is gratifying to see that the most stable species of histamine observed corresponds to that predicted to be of lowest energy (G-IVa). However, G-Ib is predicted to be higher in energy than several of the gauche conformers of the $N_{(3)}$-H tautomer, G-Vc (i.e., C/T3) being the next lowest in energy, and our plausible identification of C/T4 as G-Ic of the same tautomer implies that C/T4 should have about the same energy as C/T2. We conclude that calculations of total energies using the 3-21G basis are not quite reliable enough to use for deciding relative stabilities of conformers of the kind we are discussing here. The 6-31G-based calculations give the same trend in relative energies and improved magnitudes, but still not completely satisfactory. It seems to be very difficult to obtain quantitatively reliable relative energies for species that contain different types of internal hydrogen bondings if we do not include polarization functions in the basis.

Conclusion

By studying the rotational spectrum of gaseous histamine, we have been able to establish that the four most stable conformers are all gauche and with closely similar energies. Ab initio molecular orbital calculations proved a very useful guide to the kinds of tautomer/conformer that would be found but were not completely reliable in predicting relative energies. Although 20 tautomer/conformers were identified by the molecular orbital calculations, and we have been able to identify three of the four species, possibly the fourth, found experimentally with one gauche conformer of the $N_{(1)}$-H tautomer and three of the gauche conformers of the $N_{(3)}$-H tautomer.

Previous studies of histamine as a crystal or in solution have identified a trans conformer as the most stable, and so it is evident that this conformer is stabilized by appropriate surrounding molecules. It will be interesting to discover whether the relative stabilities of conformer/tautomers play an important role in the biological activity of histamine, although it is widely believed that it is the histaminium cation that is biologically active. To this end, we look forward to studying the shapes of complexes of histamine with one or more water molecules.

Acknowledgment. B.V. acknowledges the grant of a Nachwuchsstipendium of the Schweizerischer Nationalfonds zur Förderung der wissenschaftlichen Forschung. The research was supported by a grant from the Australian Research Council.

Registry No. Histamine, 51-45-6.

Supplementary Material Available: Listings of observed and calculated frequencies of observed lines for the four histamine species (6 pages). Ordering information is given on any current masthead page.